Inorganic Chemistry
Article

Inorg. Chem. **2011**, *50*, 873–882 **873**
DOI: 10.1021/ic101466u

Water-Soluble Cp Ruthenium Complex Containing 1,3,5-Triaza-7-phosphaadamantane and 8-Thiotheophylline Derivatives: Synthesis, Characterization, and Antiproliferative Activity

Lazhar Hajji,[†] Cristobal Saraiba-Bello,[†] Antonio Romerosa,*[,†] Gaspar Segovia-Torrente,[†] Manuel Serrano-Ruiz,[†] Paola Bergamini,[‡,§] and Alessandro Canella[∥]

[†]*Área de Química Inorgánica, Facultad de Ciencias Experimentales, Universidad de Almería, 04071 Almería, Spain,* [‡]*Dipartimento di Chimica dell'Università di Ferrara, via L. Borsari 46, 44100 Ferrara, Italia,* [§]*Consorzio Interuniversitario di Ricerca in Chimica dei Metalli nei Sistemi Biologici, Italia, and* [∥]*Dipartimento di Biochimica e Biologia Molecolare dell'Università di Ferrara, via L. Borsari 46, 44100 Ferrara, Italia*

Received July 22, 2010

The new water-soluble ruthenium(II) mononuclear complexes [RuCp(X)(PTA)(L)] (X = 8-thio-theophyllinate (TTH^-), L = PTA (**1**), L = PPh_3 (**7**)); (X = 8-methylthio-theophyllinate (8-MTT^-), L = PTA (**2**), L = PPh_3 (**8**)), (X = 8-benzylthio-theophyllinate (8-$BzTT^-$), L = PTA (**3**), L = PPh_3 (**9**)) and binuclear complexes [{RuCp(PTA)(L)}$_2$-μ-(Y-$\kappa N7,N'7$)] (Y = bis(*S*-8-thioetheophyllinate)methane ($MBTT^{2-}$), L = PTA (**4**), L = PPh_3 (**10**)), (Y = 1,2-bis(*S*-8-thioetheophyllinate)ethane ($EBTT^{2-}$), L=PTA (**5**), L=PPh_3 (**11**)), (Y=1,3-bis(*S*-8-thioetheophyllinate)propane ($PBTT^{2-}$); L=PTA (**6**), L=PPh_3 (**12**)) have been synthesized and characterized by NMR, IR spectroscopy and elemental analysis. The single crystal X-ray structure of [RuCp(8-MTT-κS)(PTA)$_2$] (**2**) was also obtained. The antiproliferative activity of the complexes on *cis*platin-sensitive T2 and *cis*platin-resistant SKOV3 cell lines has been evaluated.

Introduction

Transition metal complexes designed to bind to DNA have been extensively studied in the last few decades.[1] The discovery of the anticancer properties of *cis*platin[2] in the 1960s by Rosenberg proved that transition metal complexes could be toxic for tumor cells. As a consequence, a huge number of metal compounds of wide structural diversity have been tested and some of them found to be therapeutic agents for cancer treatment. Still now *cis*platin and its parent analogues are among the most widely used chemotherapeutic agents.[3]

Nevertheless, platinum-based drugs still present a few drawbacks like activity restricted to a limited number of tumors, severe side effects, drug resistance,[4] and so forth. Therefore the search for new metal-based drugs is still a lively field. Ruthenium complexes are promising anticancer agents[5] and two of them, NAMI-A[6] and KP1019[7] are currently under clinical trials, for the treatment of metastatic and colorectal cancers, respectively.

The cytotoxicity of ruthenium compounds, as for *cis*platin, correlates with their ability for DNA binding, which is based on the formation of metal containing active species mainly by aquation processes. It is known that Ru(III) complexes are

*To whom correspondence should be addressed. E-mail: romerosa@ual.es.

(1) (a) Farrer, N. J.; Salassa, L.; Sadler, P. J. *Dalton Trans.* **2009**, *48*, 10690–10701. (b) Foxon, S. P.; Phillips, T.; Gill, M. R.; Towrie, M.; Parker, A. W.; Webb, M.; Thomas, J. A. *Angew. Chem., Int. Ed.* **2007**, *46*, 3686. (c) Neves, A.; Lanznaster, M.; Bortoluzzi, A. J.; Peralta, R. A.; Casellato, A.; Castellano, E. E.; Herrald, P.; Riley, M. J.; Schenk, G. *J. Am. Chem. Soc.* **2007**, *129*, 7486. (d) Metcalfe, C.; Thomas, J. A. *Chem. Soc. Rev.* **2003**, *32*, 215. (e) Clarke, M. J.; Zhu, F.; Frasca, D. R. *Chem. Rev.* **1999**, *99*, 2511. (f) Zeglis, B. M.; Pierre, V. C.; Barton, J. K. *Chem. Commun.* **2007**, 4565. (g) Reedijk, J. *Proc. Natl. Acad. Sci. U. S. A.* **2003**, *100*, 3611. (h) Mestroni, G.; Alessio, E.; Sava, G.; Pacor, S.; Coluccia, M.; Boccarelli, A. *Met.-Based Drugs* **1994**, *1*, 41. (i) Coluccia, M.; Sava, G.; Loseto, F.; Nassi, A.; Boccarelli, A.; Giordano, D.; Alessio, E.; Mestroni, G. *Eur. J. Cancer* **1993**, *29*, 1873.

(2) Rosenberg, B.; van Camp, L.; Krigas, T. *Nature* **1965**, *205*, 698.

(3) Jamieson, E. R.; Lippard, S. J. *Chem. Rev.* **1999**, *99*, 2467.

(4) Stordal, B.; Davey, M. *IUBMB Life* **2007**, *59*, 696. Pabla, N.; Dong, Z. *Kidney Int.* **2008**, *73*, 994.

(5) (a) Betanzos-Lara, S.; Salassa, L.; Habtemariam, A.; Sadler, P. J. *Chem. Commun.* **2009**, 6622–6624. (b) Pascu, G. I.; Hotze, A. C. G.; Sanchez-Cano, C.; Kariuki, B. M.; Hannon, M. J. *Angew. Chem., Int. Ed.* **2007**, *46*, 4374. (c) Ang, W. H.; Dyson, P. J. *Eur. J. Inorg. Chem.* **2006**, 4003–4018. (d) Yan, Y. K.; Melchart, M.; Habtemariam, A.; Sadler, P. J. *Chem. Commun.* **2005**, 4764. (e) Hotze, A. C. G.; Caspers, S. E.; de Vos, D.; Kooijman, H.; Spek, A. L.; Flamigni, A.; Bacac, M.; Sava, G.; Haasnoot, J. G.; Reedijk, J. *J. Biol. Inorg. Chem.* **2004**, *9*, 354. (f) Morris, R. E.; Sadler, P. J.; Chen, H.; Jodrell, D. U.S. Patent 6 750 251 B2, 2004.

(6) (a) Alessio, E.; Mestroni, G.; Bergamo, A.; Sava, G. *Curr. Top. Med. Chem.* **2004**, *4*, 1525. (b) Alessio, E.; Mestroni, G.; Bergamo, A.; Sava, G. *Met. Ions Biol. Syst.* **2004**, *42*, 323.

(7) Hartinger, C. G.; Zorbas-Selfried, S.; Jakupee, M. A.; Kynast, B.; Zorbas, H.; Keppler, B. K. *J. Inorg. Biochem.* **2006**, *100*, 891.

Published on Web 01/12/2011

Chart 1

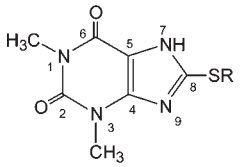

R = H, 8-TTH$_2$, **a**
R = Me, 8- MTTH, **b**
R = CH_2Ph, 8- BzTTH, **c**

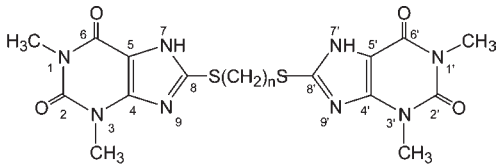

n = 1, MBTTH$_2$, **d**
n = 2, EBTTH$_2$, **e**
n = 3, PBTTH$_2$, **f**

relatively inert toward ligand substitution and therefore their anticancer activity depends on the ease of reduction to more labile Ru(II) complexes.[8] As a consequence, organometallic ruthenium(II) compounds attracted the attention of drug designers in their search for novel antiproliferative agents. The use of arene ligands, which stabilize ruthenium in the +2 oxidation state, initiated a new phase in the search for ruthenium anticancer drugs.

Additionally, proteins, peptides, and also some small molecules can play significant roles in the anticancer activity and resistance to drugs.[9] Among biomolecules, sulfur-containing proteins are of special interest for their abundance and their high affinity for platinum and ruthenium (e.g., albumin).[10] An important example of this family of proteins is the copper transporter protein CTR1 that appears to be involved in platinum-drug transport through the cell membrane.[11] The S-donor molecules seem to play a relevant role in the anticancer activity of platinum complexes of *trans* geometry acting with a different mechanism with respect to traditional *cis*platin complexes.[12] Furthermore, it is possible to exploit sulfur oxidation as a mechanism for the activation of Ru(II) arene thiolate pro-drugs as well as for the reactivation of metabolites of Ru(II) arene anticancer drugs,[13] which are sometimes controlled by metal complexation to the S atom of proteins and enzymes.[14] Thiolate oxygenation seems to activate cytotoxic half-sandwich $[(\eta^6\text{-arene})Ru(en)(SR)]^+$ complexes (en = ethylenediamine; arene = *p*-cymene, hexamethylbenzene; SR = alkyl or aryl thiolate) toward DNA binding and the properties of Ru−S bonds depend on the extent of S oxygenation, on the nature of the thiolate substituent and of the arene group.[15]

We have recently published the synthesis and interaction with DNA of the Ru(II) piano-stool complexes $[RuCpX(PR^1{}_3)(PR^2{}_3)]$ (X = Cl, I; $PR^1{}_3 = PPh_3$; $PR^2{}_3$ = PTA, mPTA; $PR^1{}_3 = PR^2{}_3$ = PTA, mPTA) (PTA = 1,3,5-triaza-7-phosphaadamantane; mPTA = *N*-methyl-1,3,5-triaza-7-phosphaadamantane).[16] The DNA binding activity of these complexes was found dependent on the ligand bonded to the metal, the ones containing chloride being active agents while the iodide analogues are inactive. The DNA binding activity was also dependent on which phosphine is coordinated to the metal, PTA or mPTA. Therefore the interaction of the biologically active $[RuCpX(PR^1{}_3)(PR^2{}_3)]$ (X = halogens) species with DNA can be favored and maximized by an appropriate combination of hydro and liposoluble phosphines and by the adequate choice of the anionic ligand X.

Looking for biologically active metal complexes, a few years ago we studied a group of Pt-phosphines complexes bearing the deprotonated form of the 8-thiotheophylline derivatives **b**−**f** depicted in Chart 1 as anionic ligands.[17]

We showed that Pt complexes containing PPh_3 and the N7 coordinated anionic thiopurinic ligand 8-MTT$^-$ show a remarkable antiproliferative activity on some human cancer cell lines. Following the hypothesis that such activity could be improved by modulating the lipo-hydrophilicity of the coordinated phosphines, we tested the PTA analogues and also a series of PTA/PPh_3 dinuclear Pt complexes of the bis-thiopurines bis(*S*-8-thiotheophylline)methane (MBTTH$_2$; Chart 1, **d**), 1,2-bis(*S*-8-thiotheophylline)ethane (EBTTH$_2$; Chart 1, **e**), and 1,3-bis(*S*-8-thiotheophylline)propane (PBTTH$_2$; Chart 1, **f**). We found that the platinum complexes containing both PTA and PPh_3, a hydrophilic and a lipophilic phosphine, display on model tumoral cell lines T2 and SKOV3 an antiproliferative activity better than the analogues containing a single phosphine type, probably because of a more favorable balance between lipophilicity and hydrophilicity of the entire complex.[18] Referring to such promising results obtained on platinum, as the next step we planned to extend the study of the favorable combination to ruthenium complexes of thiopurinic and phosphinic PTA and PPh_3 ligands. It is reasonable to suppose that the substitution of the chloride ligand in $[RuCpCl(PR^1{}_3)(PR^2{}_3)]$ complexes ($PR^1{}_3 = PPh_3$; $PR^2{}_3$ = PTA) by a thiopurine could enhance the antiproliferative activity of the parent complexes. Moreover, this study could provide additional information on the interaction of ruthenium complexes with purines.

(8) Clarke, M. J. *Coord. Chem. Rev.* **2003**, *236*, 209.
(9) (a) Jung, Y. W.; Lippard, S. J. *Chem. Rev.* **2007**, *107*, 1387. (b) Kuo, M. T.; Chen, H. H.W.; Song, I. S.; Savaraj, N.; Ishikawa, T. *Cancer Metastasis Rev.* **2007**, *26*, 71. (c) Martin, L. P.; Hamilton, T. C.; Schilder, R. J. *Clin. Cancer Res.* **2008**, *14*, 1291.
(10) (a) Ivanov, A. I.; Christodoulou, J.; Parkinson, J. A.; Barnham, K. J.; Tucker, A.; Woodrow, J.; Sadler, P. J. *J. Biol. Chem.* **1998**, *273*, 14721. (b) Montero, E. I.; Benedetti, B. T.; Mangrum, J. B.; Oehlsen, M. J.; Qu, Y.; Farrell, N. P. *Dalton Trans.* **2007**, 4938.
(11) Arnesano, F.; Scintilla, S.; Natile, G. *Angew. Chem., Int. Ed.* **2007**, *46*, 9062.
(12) Li, C.; Li, Z.; Sletten, E.; Arnesano, F.; Losacco, M.; Natile, G.; Liu, Y. *Angew. Chem., Int. Ed.* **2009**, *48*, 8497.
(13) (a) Charles, R. L.; Schroder, E.; May, G.; Free, P.; Gaffney, P. R. J.; Wait, R.; Begum, S.; Heads, R. J.; Eaton, P. *Mol. Cell. Proteomics* **2007**, *6*, 1473. (b) Jacob, C.; Knight, I.; Winyard, P. G. *Biol. Chem.* **2006**, *387*, 1385–1397.
(14) (a) Maret, W. *Antioxid. Redox Signaling* **2006**, *8*, 1419–1441. (b) Dey, A.; Jeffrey, S. P.; Darensbourg, M.; Hodgson, K. O.; Hedman, B.; Solomon, E. I. *Inorg. Chem.* **2007**, *46*, 4989–4996.
(15) Sriskandakumar, T.; Petzold, H.; Bruijnincx, P. C. A.; Habtemariam, A.; Sadler, P. J.; Kennepohl, P. *J. Am. Chem. Soc.* **2009**, *131*, 13355–13361.
(16) Romerosa, A.; Campos-Malpartida, T.; Lidrissi, C.; Saoud, M.; Serrano-Ruiz, M.; Peruzzini, M.; Garrido-Cardenas, J. A.; Garcia-Maroto, F. *Inorg. Chem.* **2006**, *45*, 1289–1298.
(17) Romerosa, A.; Bergamini, P.; Bertolasi, V.; Canella, A.; Cattabriga, M.; Gavioli, R.; Mañas, S.; Mantovani, N.; Pellacani, L. *Inorg. Chem.* **2004**, *43*, 905–913.
(18) Bergamini, P.; Bertolasi, V.; Marvellli, L.; Canella, A.; Gavioli, R.; Mantovani, N.; Mañas, S.; Romerosa, A. *Inorg. Chem.* **2007**, *46*, 4267–4276.

In this paper we present the synthesis and characterization of a new family of water-soluble neutral mononuclear ruthenium complexes [RuCp(X)(PR^1_3)(PR^2_3)] (X = 8-thioteophyllinate (TTH^-; Chart 1, **a**), 8-methyl-thio-teophyllinate (8-MTT^-; Chart 1, **b**), 8-benzyl-thio-theophyllinate (8-$BzTT^-$; Chart 1, **c**) and binuclear ruthenium complexes [{RuCp(L)(L′)}$_2$-μ-(Y-$\kappa N7,N'7$)] (Y = bis-thiopurines-bis-(*S*-8-thiotheophyllinate)methane ($MBTT^{2-}$; Chart 1, **d**), 1, 2-bis(*S*-8-thiotheophyllinate)ethane ($EBTT^{2-}$; Chart 1, **e**), 1,3-bis(*S*-8-thiotheophyllinate)propane ($PBTT^{2-}$; Chart 1, **f**) with two coordinated PTA ((PR^1_3 = PR^2_3 = PTA) or one PPh_3 and one PTA (PR^1_3 = PPh_3; PR^2_3 = PTA) and their antiproliferative activity on *cis*platin-sensitive T2 and *cis*platin-resistant SKOV3 model cell lines.

Experimental Section

General Procedures. All chemicals were reagent grade and were used as received by commercial suppliers unless otherwise stated. The solvents were all degassed and distilled according to standard procedures.[19] All reactions and manipulations were routinely performed under a dry nitrogen atmosphere by using standard Schlenk-tube techniques. The compounds PTA, [RuClCp(PTA)$_2$], and [RuClCp(PPh_3)(PTA)] were prepared as described in the literature.[16,20,21] Ligands 8-thiotheophylline (8-TTH_2), 8-methylthiotheophylline (8-MTTH), 8-benzylthiotheophylline (8-BzTTH), bis(*S*-8-thiotheophylline)methane ($MBTTH_2$), 1,2-bis(*S*-8-thiotheophylline)ethane ($EBTTH_2$), 1,3-bis(*S*-8-thiotheophylline)propane ($PBTTH_2$) have been prepared following the procedure described by literature methods.[22,23] ^{1}H, ^{31}P{^{1}H} NMR, and ^{13}C{^{1}H} NMR spectra were recorded on a Bruker DRX300 spectrometer operating at 300.13 MHz (^{1}H), 121.49 MHz (^{31}P), and 75.47 MHz (^{13}C), respectively. Peak positions are relative to tetramethylsilane and were calibrated against the residual solvent resonance (^{1}H) or the deuterated solvent multiplet (^{13}C). Chemical shifts for ^{31}P-{^{1}H} NMR were measured relative to external 85% H_3PO_4 with downfield values taken as positive. The ^{1}H,^{1}H-2D COSY NMR experiments were routinely conducted on the Bruker DRX300 instruments in the absolute magnitude mode using a 45 or 90° pulse after the incremental delay. Infrared spectra were recorded on KBr discs using an FT-IR ATI Mattson Infinity Series. Elemental analysis (C, H, N, S) were performed on a Fisons Instruments EA 1108 elemental analyzer.

Synthesis of [RuCp(8-TTH-κS)(PTA)$_2$] (1). The ligand 8-TTH_2 (0.074 g, 0.35 mmol) was dissolved into 10 mL of degassed aqueous KOH solution (0.035 M) and stirred for 15 min. The complex [RuClCp(PTA)$_2$] (0.180 g, 0.35 mmol) was added, and the resulting solution kept at refluxing temperature for 4 h. The obtained solution was concentrated under reduced pressure until 1 mL. The yellow precipitate obtained was filtered and washed with EtOH (2 × 2 mL) and Et_2O (2 × 2 mL), and vacuum-dried.

Yield: 0.170 g, 68%. S_{25}(mg/cm^3): 18. Log *P*: −1.29. Elemental analysis for $C_{24}H_{36}N_{10}O_2P_2RuS$ (691.69): Found C, 41.75; H, 5.33; N, 20.10; S, 4.47%; calcd. C, 41.67; H, 5.25; N, 20.25; S, 4.64%.

Synthesis of [RuCp(8-MTT-κS)(PTA)$_2$] (2). Complex **2** was prepared in the same way as **1** but using the 8-MTTH (0.079 g, 0.35 mmol) as the purine derivate. The product was obtained as a yellow powder. Good quality yellow crystals for X-ray diffraction were obtained by slow evaporation from an EtOH solution of **2**.

Yield: 0.190 g, 75%. S_{25}(mg/cm^3): 32. Log *P*: −1.41. Elemental analysis for $C_{25}H_{38}N_{10}O_2P_2RuS$ (705.72): Found C, 42.64; H, 5.52; N, 19.68; S, 4.40%; calcd. C, 42.55; H, 5.43; N, 19.85; S, 4.54%.

Synthesis of [RuCp(8-BzTT-κS)(PTA)$_2$] (3). The procedure used for the synthesis of the complex **3** was similar to that described for **1**. The 8-BzTTH (0.105 g, 0.35 mmol) was dissolved into 10 mL of aqueous KOH solution (0.035 M), stirred for 15 min, and [RuClCp(PTA)$_2$] (0.180 g, 0.35 mmol) was added. The product was obtained as a yellow powder.

Yield: 0.220 g, 78%. S_{25}(mg/cm^3): 38. Log *P*: −0.97. Elemental analysis for $C_{31}H_{42}N_{10}O_2P_2RuS$ (781.81): Found C, 47.62; H, 5.52; N, 17.76; S, 3.91%; calcd. C, 47.62; H, 5.41; N, 17.92; S, 4.10%.

Synthesis of [{RuCp(PTA)$_2$}$_2$(μ-MBTT-$\kappa N7,N'7$)] (4). The bis-thiopurine $MBTTH_2$ (15.0 mg, 0.034 mmol) was introduced into a 10 mL deoxygenated aqueous KOH solution (0.0068 M). The mixture was stirred until complete dissolution of $MBTTH_2$ and then [RuClCp(PTA)$_2$] (35.5 mg, 0.068 mmol) was added. The mixture was refluxed for 4 h, cooled, filtered, and concentrated by evaporation to 2 mL. The obtained precipitate was filtered, washed with EtOH (2 × 1 mL) and Et_2O (2 × 2 mL), and dried under vacuum.

Yield: 43.0 mg, 85%. S_{25}(mg/cm^3): 57. Log *P*: −1.55. Elemental analysis for $C_{49}H_{72}N_{20}O_4P_4Ru_2S_2$ (1395.40): Found C, 42.30; H, 5.25; N, 19.91; S, 4.42%; calcd. C, 42.30; H, 5.25; N, 19.91; S, 4.42%.

Synthesis of [{RuCp(PTA)$_2$}$_2$(μ-EBTT-$\kappa N7,N'7$)] (5). The synthesis of complex **5** was carried out by a similar procedure to that described for **4**. In this case, the ligand $EBTTH_2$ (15.0 mg, 0.032 mmol) was dissolved into a deoxygenated aqueous KOH solution (10 mL, 0.0064 M) and [RuClCp(PTA)$_2$] (33.5 mg, 0.064 mmol) was added. The product was separated as a yellow powder.

Yield: 30 mg, 62.0%. S_{25}(mg/cm^3): 40. Log *P*: −1.47. Elemental analysis for $C_{50}H_{74}N_{20}O_4P_4Ru_2S_2$ (1409.42): Found C, 43.10; H, 5.51; N, 19.50; S, 4.38%; calcd. C, 42.61; H, 5.29; N, 19.88; S, 4.55%.

Synthesis of [{RuCp(PTA)$_2$}$_2$(μ-PBTT-$\kappa N7,N'7$)] (6). The bis-thiopurine $PBTTH_2$ (15.0 mg, 0.031 mmol) dissolved in 10 mL deoxygenated aqueous KOH solution (0.0062 M) reacted with [RuClCp(PTA)$_2$] (32.5 mg, 0.062 mmol) to give, after the same work up as above, complex **6** as a yellow powder.

Yield: 33 mg, 70%. S_{25}(mg/cm^3): 36. Log *P*: −1.42. Elemental analysis for $C_{51}H_{76}N_{20}O_4P_4Ru_2S_2$ (1423.45): Found C, 43.10; H, 5.51; N, 19.50; S, 4.38%; calcd. C, 43.03; H, 5.38; N, 19.68; S, 4.51%.

Synthesis of [RuCp(8-TTH-κS)(PPh_3)(PTA)] (7). The complex [RuClCp(PPh_3)(PTA)] (0.150 g, 0.24 mmol) was added to a solution of the ligand 8-TTH_2 (0.051 g, 0.24 mmol) in 10 mL of ethanolic KOH (0.024 M). The mixture refluxed and stirred for 4 h, cooled down to room temperature, and concentrated under reduced pressure to 1 mL. The resulting yellow precipitate was washed with EtOH (2 × 2 mL) and Et_2O (2 × 2 mL), and vacuum-dried.

Yield: 0.160 g, 84%. S_{25}(mg/cm^3): 0.8. Log *P*: 0.96. Elemental analysis for $C_{36}H_{39}N_7O_2P_2RuS$ (796.82): Found C, 54.35; H, 5.05; N, 12.25; S, 4.02%; calcd. C, 54.26; H, 4.93; N, 12.30; S, 4.02%.

Synthesis of [RuCp(8-MTT-κS)(PPh_3)(PTA)] (8). The yellow complex **8** was obtained by the procedure described above for **7**.

(19) *Purification of Laboratory Chemicals*, 3rd ed.; Perrin, D. D.; Armarego, W. L. F., Eds.; Butterworths and Heinemann: Oxford, 1988.

(20) *Aqueous-Phase Organometallic Catalysis*; Cornils, B.; Herrmann, W. A., Eds.; Wiley-VCH: Weinheim, Germany, 1998.

(21) Joó, F.; Kovacs, J.; Katho, A.; Benyei, A. C.; Decuir, T.; Darensboug, D. J. *Inorg. Synth.* **1998**, *32*, 2.

(22) Romerosa, A.; López-Magaña, C.; Goeta, A. E.; Mañas, S.; Saoud, M.; Benbdelouahab, F. B.; El Guemmout, F. *Inorg. Chim. Acta* **2003**, *353*, 99–106.

(23) (a) Romerosa, A.; López-Magaña, C.; Saoud, M.; Colacio, E.; Suárez-Varela, J. *Inorg. Chim. Acta* **2000**, *307*, 125–130. (b) Romerosa, A.; López-Magaña, C.; Saoud, M.; Mañas, S. *Eur. J. Inorg. Chem.* **2003**, 348–355. (c) Romerosa, A.; López-Magaña, C.; Mañas, S.; Saoud, M.; Goeta, A. E. *Inorg. Chim. Acta* **2003**, *353*, 145–150.

The 8-MTTH (0.055 g, 0.24 mmol) was used as the purine derivate and reacted with [RuClCp(PPh_3)(PTA)] (0.150 g, 0.24 mmol) in 10 mL of an ethanolic solution of KOH (0.024 M).

Yield: 0.140 g, 70%. S_{25}(mg/cm^3): 1.1. Log *P*: 1.26. Elemental analysis for $C_{37}H_{41}N_7O_2P_2RuS$ (810.85): Found C, 54.87; H, 5.17; N, 12.02; S, 3.87%; calcd. C, 54.81; H, 5.10; N, 12.09; S, 3.95%.

Synthesis of [RuCp(8-BzTT-κ*S*)(PPh_3)(PTA)] (9). The complex **9** was obtained as a yellow powder by the procedure described above for **7**. The ligand 8-BzTTH (0.072 g, 0.24 mmol) was reacted with [RuClCp(PPh_3)(PTA)] (0.150 g, 0.24 mmol) in 10 mL of an ethanolic solution of KOH (0.024 M).

Powder yield: 0.150 g, 70%. S_{25}(mg/cm^3): 1.3. Log *P*: 1.54. Elemental analysis for $C_{43}H_{45}N_7O_2P_2RuS$ (886.95): Found C, 58.32; H, 5.16; N, 10.87; S, 3.48%; calcd. C, 58.23; H, 5.11; N, 11.05; S, 3.62%.

Synthesis of [{RuCp(PPh_3)(PTA)}$_2$(μ-MBTT-κ*N7,N′7*)] (10). The ligand $MBTTH_2$ (10.0 mg, 0.022 mmol) was dissolved in 10 mL of a KOH ethanolic solution (0.0044 M) and reacted with [RuClCp(PPh_3)(PTA)] (28.4 mg, 0.044 mmol). After refluxing for 4 h the resulting solution was filtered at room temperature and concentrated under reduced pressure to 2 mL. The produced precipitate was filtered, washed with Et_2O (2 × 2 mL), and finally dried under vacuum.

Yield: 33.4 mg, 88.4%. S_{25}(mg/cm^3): 0.8. Log *P*: 0.63. Elemental analysis for $C_{73}H_{88}N_{14}O_4P_4Ru_2S_2$ (1615.74): Found C, 54.35; H, 5.58; N, 12.02; S, 3.82%; calcd. C, 54.27; H, 5.49; N, 12.14; S, 3.97%.

Synthesis of [{RuCp(PPh_3)(PTA)}$_2$(μ-EBTT-κ*N7,N′7*)] (11). The same procedure described above for **10** was used. The purine derivative $EBTTH_2$ (10.4 mg, 0.022 mmol) was reacted with [RuClCp($PTA)_2$] (28.4 mg, 0.044 mmol) to give **11** as a yellow powder.

Yield: 29.6 mg, 78%. S_{25}(mg/cm^3): 0.8. Log *P*: 0.78. Elemental analysis for $C_{74}H_{90}N_{14}O_4P_4Ru_2S_2$ (1629.77): Found C, 54.57; H, 5.64; N, 11.92; S, 3.86%; calcd. C, 54.53; H, 5.57; N, 12.03; S, 3.94%.

Synthesis of [{RuCp(PPh_3)(PTA)}$_2$(μ-PBTT-κ*N7,N′7*)] (12). The purine derivative $PBTTH_2$ (10.5 mg, 0.022 mmol) was reacted with [RuClCp($PTA)_2$] (28.4 mg, 0.044 mmol) to give **12** as a yellow powder by using a similar procedure as that described for **10**.

Yield: 26 mg, 67.7%. S_{25}(mg/cm^3): 0.6. Log *P*: 1.12. Elemental analysis for $C_{75}H_{92}N_{14}O_4P_4Ru_2S_2$ (1643.79): Found C, 54.87; H, 5.75; N, 11.77; S, 3.77%; calcd. C, 54.80; H, 5.64; N, 11.93; S, 3.90%.

Stability Tests of the Complexes with O_2 and H_2O. The obtained ruthenium complexes were air stable for months in the solid state and for 2 days in solution. In a standard procedure, 0.01 g of **1**−**6**, **7**−**10** and **12**, and **11** were introduced into a 5 mm NMR tube and dissolved respectively in D_2O, $CDCl_3$, and DMSO-d_6 (1.0 mL). The solution was cooled to 0 °C and then dry O_2 was bubbled throughout the solution for 2 min via a long syringe needle. $^{31}P\{^1H\}$ NMR monitoring showed no change within 2 days at room temperature. No decomposition was also observed after 2 days at 40 °C as well. Introduction of 50 μL of D_2O in the $CDCl_3$ and DMSO-d_6 solutions did not produced any significant change in the starting complexes after 2 days at 40 °C.

X-ray Structure Determinations. Data of compounds **2**·4H_2O was collected on a Bruker APEX CCD diffractometer (XDIFRACT service of the University of Almería) using graphite monochromated Mo Kα radiation (λ = 0.7107 Å) at 150 K. The crystal parameters and other experimental details of the data collections are summarized in Table 1. The structures were solved by direct methods SIR92[24] and refined by full-matrix least-squares methods with SHEL-XTL[25] and refined by least-squares procedures on F^2 and final geometrical calculations and graphical manipulations were carried our with the SHELXS-XTL package.[25] A disordered solvent molecule H_2O was found and refined isotropically. All the non-hydrogen non-disordered atoms were refined with anisotropic atomic displacement parameters. All hydrogen atoms, except for disordered water molecules, were included in calculated positions and refined using a riding model.

Table 1. Crystallographic Data for **2**·4H_2O

	2·4H_2O
formula	$C_{25}H_{46}N_{10}O_6P_2RuS$
M_r	769.72
space group	$P\bar{1}$
cryst system	triclinic
a/Å	10.6102(5)
b/Å	11.9397(6)
c/Å	12.7843(7)
α/deg	99.4780(10)
β/deg	90.3920(10)
γ/deg	90.4700(10)
V/Å^3	1597.33(14)
Z	2
D_c/g cm^{-3}	1.600
F(000)	792
M(Mo Kα)/cm^{-1}	7.13
measd reflctns	8423
unique reflctns	5223
R_{int}	0.0564
obsd reflctns [$I \geq 2\sigma(I)$]	4436
$\theta_{min}-\theta_{max}$/deg	1.61−24.41
hkl ranges	−12, 12; −13, 13; −11, 14
$R(F^2)$ (obsd reflctns)	0.0423
$wR(F^2)$ (all reflctns)	0.1620
no. of variables	436
goodnes of fit	1.095
ρ_{min}, ρ_{max}/e Å^{-3}	−0.898, 0.800

Growth Inhibition Assays. Cell growth inhibition assays were carried out using the *cis*platin-sensitive T2 human cell line and the *cis*platin-resistant SKOV3 cell line. T2 is a cell hybrid obtained by the fusion of the human lymphoblastoid line 174 (B lymphocyte transformed by the Epstein−Barr virus) with the CEM human cancer line (leukemia T) while SKOV3 is derived from a human ovarian tumor. The cells were seeded in triplicate in 96-well trays at a density of 50 × 10^3 in 50 μL of AIM-V medium for T2, 25 × 10^3 in 50 μL of AIM-V medium for SKOV3. Stock solutions (10 mM) of the Ruthenium complexes **1**−**12** were made in dimethylsulfoxide (DMSO) and diluted in AIM-V medium to give a final concentration of 2, 10, and 50 μM. *Cis*platin was employed as a control for the *cis*platin-sensitive T2 cell line and for the *cis*platin-resistant SKOV3. Untreated cells were placed in every plate as a negative control. The cells were exposed to the compounds for 72 h, and then 25 μL of a 4,5-dimethylthiozol-2-yl)2,5-diphenyltetrazolium bromide solution (12 mM) were added. After 2 h of incubation, 100 μL of lysing buffer (50% DMF + 20% SDS, pH 4.7) were added to convert 4,5-dimethylthiazol-2-yl-2,5-diphenyltetrazolium bromide into a brown colored formazane. After additional 18 h the solution absorbance, proportional to the number of live cells, was measured by a spectrophotometer and converted in % of growth inhibition.[26]

Octanol−Water Partition Coefficient Determination. The octanol−water partition coefficient of the ruthenium complexes was obtained by a slow-stirring method that provides accurate Log *P* results over a wide range of concentration values.[27]

(24) Altomare, A.; Cascarano, G.; Giacovazzo, C.; Guagliardi, A.; Burla, M. C.; Polidori, G.; Camalli, M. *J. Appl. Crystallogr.* **1994**, *27*, 435.

(25) Sheldrick, G. M. *SHELXTL*, version 6.14; Bruker-AXS: Madison, WI, 2003.

(26) Hansen, M. B.; Nielsen, S. E.; Berg, K. J. *Immunol. Methods* **1989**, *119*, 203.

Scheme 1. Synthesis of Complex **1**

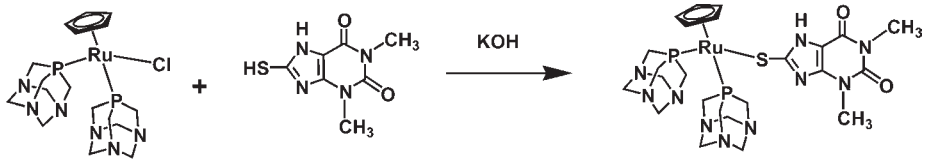

(**1**)

The procedure was adapted to the solubility properties of the complexes. The aqua-soluble ruthenium complexes **1**−**6** were previously dissolved in 15 mL of distilled water presaturated with 1-octanol while water insoluble complexes **7**−**12** in 15 mL of octanol previously saturated with distilled water. The final complex concentration of the resulting solutions lay in the range between 10^{-4} and 10^{-3} M. Into a 40 mL container with a magnetic stir bar was introduced initially the water phase and then by a syringe the octanol one so that the solution did not emulsify. The container was closed with a silicone septum and stirred slowly at 25 ± 1 °C. Samples were taken from the octanol and water phases with a syringe through the septum. Samples of each phase were taken periodically until the concentrations in both phases stabilized. Concentrations of the complex in each phase were measured using UV−vis spectroscopy.

Results and Discussions

Mononuclear Complexes Containing Monothiopurines: Synthesis of 1, 2, 3 and 7, 8, 9. The reaction of 8-TTH_2 with KOH and [RuClCp($PTA)_2$] in water at refluxing temperature gave complex [RuCp(8-TTH-κS)($PTA)_2$] (**1**) as a microcrystalline yellow powder (Scheme 1). The elemental analysis, IR, and NMR analysis support the proposed structure for **1**, in which a ruthenium atom is coordinated to a η^5-Cp, two PTA ligands, and to a 8-TTH^- purine molecule acting as an anionic monodentate ligand through its deprotonated sulfur atom.

The presence of the S-coordinated thiopurine is evidenced by the characteristic IR spectrum absorption for ν(C6=O + C2=O) at 1690 and 1636 cm^{-1}, for ν(C=C + C=N) at 1536 cm^{-1} and for ν(N−H) at 3419 cm^{-1}. The ^{1}H NMR spectrum in D_2O displays two singlets at 3.15 ppm and 3.32 ppm that are ascribable to the N1-$CH_{3(8\text{-TTH})}$ and N3-$CH_{3(8\text{-TTH})}$ for a coordinate TTH^-. The N7−H signal was not observed. The lack of N7−H signal is probably due to rapid deuterium exchange in D_2O. Unfortunately **1** is not soluble in any aprotic solvent like $CDCl_3$, where this exchange process does not occur. The characteristic $NCH_2P_{(PTA)}$ and $NCH_2N_{(PTA)}$ signals are observed in the range 3.84−4.18 ppm and 4.38−4.55 ppm, respectively. The singlet of the Cp ligand is found at 4.82 ppm. The $^{13}C\{^1H\}$ NMR spectrum is in agreement with the proposed composition: signals for N1-$CH_{3(8\text{-TTH})}$ and N3-$CH_{3(8\text{-TTH})}$ thiopurine methyl groups and for the Cp ligand are observed at 27.97 ppm, 30.19 ppm, and 79.49 ppm, respectively. The chemical shift for the C8−S carbon atom arises at 158.89 ppm, at higher field than that found for 8-TTH_2 in the same solvent (164.83 ppm).[22,23] Unfortunately the chemical shift of C8−S has not been reported for analogue complexes. The presence of coordinated PTA is also supported, in the $^{31}P\{^1H\}$ NMR spectrum, by a singlet at −22.97 ppm whose chemical shift is similar to that observed for the PTA ligand in [RuClCp($PTA)_2$] (−23.6 ppm).[28]

Chart 2. Structure of [RuCp(8-MTT-κS)($PTA)_2$]

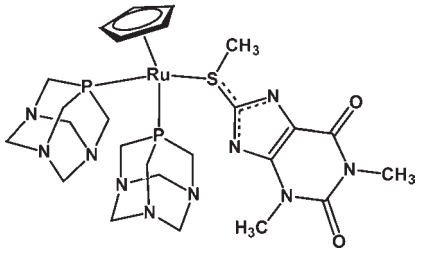

Complex **2** was obtained from the reaction between 8-MTTH, KOH, and [RuClCp($PTA)_2$] in water. The spectroscopic data suggested that the structure of **2** was similar to other previously reported 8-MTT^- metal complexes. Its IR spectrum showed no ν(N−H) absorption band but absorptions for ν(C6=O + C2=O) (1677, 1628 cm^{-1}) and ν(C=C + C=N) (1519 cm^{-1}) in the range found for 8-MTT^- complexes in which the purine is bonded to the metal by the imidazolic N7 atom.[17,18,22,23a] ^{1}H, ^{13}C, and ^{31}P NMR spectra of **2** in $CDCl_3$ showed a single pattern, excluding the formation of isomers. The ^{1}H NMR displayed the expected signals for a Cp, two PTA, and an 8-MTT^-. It is important to point out that the singlet at 2.75 ppm for S-CH_3 is close to that reported for *cis*-[PtCl(8-MTT-$\kappa N7$)($PPh_3)_2$] (2.70 ppm).[17] The $^{13}C\{^1H\}$ NMR was also in agreement with the proposed composition for **2**. The signal for the S-CH_3 arises at 14.15 ppm that is close to that for 8-MTTH (14.00 ppm).[22,23] The $^{31}P\{^1H\}$ NMR spectrum showed a single signal at −25.19 ppm due to phosphorus-coordinated PTA. Therefore, the spectroscopic data for **2** are similar to the corresponding found in previously reported 8-MTT^- complexes where the thiopurine is invariably coordinated by the imidazolic N7. This fact suggests that in **2** the 8-MTT^- is also coordinated by the N7 atom to the metal atom of the moiety $\{RuCp(PTA)_2\}^+$.

Surprisingly, the crystal structure of **2** obtained by single crystal X-ray crystallography showed that in this complex the MTT^- ligand is coordinated to the metal by the S atom instead of the expected N7 imidazolic atom (Chart 2). The ruthenium-coordinated S atom is still bonded both to C8 and CH_3 acting therefore as a coordinated thio-ethereal group, where sulfur is triply bonded. The ligand MTT^- acts as a monodentate anionic

(27) (a) Mannhold, R.; Poda, G. I.; Ostermann, C.; Tetko, I. G. *J. Pharm. Sci.* **2009**, *98*, 861–893. (b) Lozano, H. R.; Martķnez, F. *Braz. J. Pharm. Sci.* **2006**, *42*, 601–613. (c) Ropel, L.; Belvèze, L. S.; Aki, S. N. V. K.; Stadtherr, M. A.; Brennecke, J. F. *Green. Chem.* **2005**, *7*, 83–90.

(28) Akbayeva, D. N.; Gonsalvi, L.; Oberhauser, W.; Peruzzini, M.; Vizza, F.; Brüggeller, P.; Romerosa, A.; Sava, G.; Bergamo, A. *Chem. Commun.* **2003**, 264.

Scheme 2. Synthesis of **2** and **3**

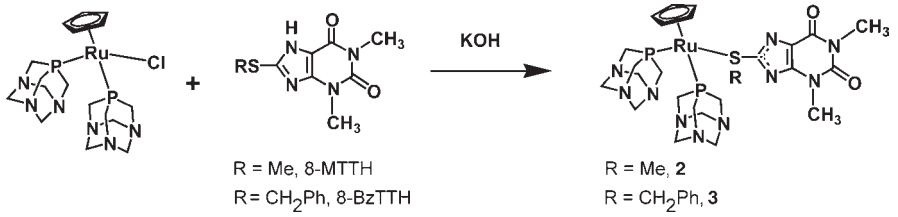

Scheme 3. Synthesis of **7**, **8**, and **9**

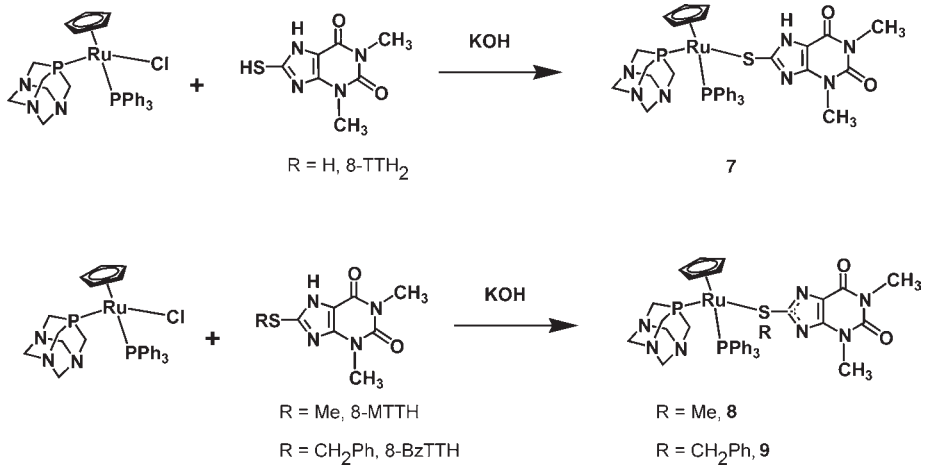

S-donor ligand, and this unusual coordination mode is not stabilized by any chelate formation.

Although it is reasonable to ascribe the observed complete regioselectivity for S versus N7 coordination to the preference of the soft acid {PTA-Ru(II)} for the soft S-donor, it must be noticed that the same behavior was not observed with {PTA-Pt(II)} (also classified as a soft acid), which was reported to form exclusively Pt−N7 bonds with MTT^-.[17,18]

The complex [RuCp(8-BzTT)$(PTA)_2$] (**3**) was obtained by a procedure similar to that used for **2**. The reaction of 8-BzTTH with KOH and [RuClCp$(PTA)_2$] in water under an inert atmosphere led to **3** (Scheme 2). The IR spectrum showed the typical bands of a coordinated thiopurine and the lack of ν(N7H) absorption. Also in this case, the NMR analysis showed a single pattern for every observed nucleus, indicating the complete regioselectivity of the coordination process. The ^{1}H NMR is constituted by the characteristic signals for PTA, Cp, and the thiopurine. The chemical shift for the S-CH_2-Ph signal (5.03 ppm) is between that found in [PdCl(8-BzTT-$\kappa N7$)$(PPh_3)_2$] (4.15 ppm) and [Pd(8-BzTT-$\kappa N7$)$_2$-$(PPh_3)_2$] (5.20 ppm), the only reported metal complexes of $BzTT^-$, and close to that for free 8-BzTTH (4.49 ppm).[23c] In $^{13}C\{^1H\}$ NMR, the chemical shifts of S-CH_2-Ph and C8-S carbon atoms are at 37.18 ppm and 150.50 ppm, close to the corresponding observed for [PdCl(8-BzTT)-$(PPh_3)_2$] (36.30 ppm; 150.2 ppm) and [Pd(8-BzTT)$_2$-$(PPh_3)_2$] (40.80 ppm; 148.4 ppm).[23c] In the $^{31}P\{^1H\}$ NMR a singlet comes at −25.88 ppm, close to those observed for [RuClCp$(PTA)_2$] (−23.6 ppm), **1** (−22.29 ppm), and **2** (−25.19 ppm). The spectroscopic properties of **3** are similar to those found for parent and analogue complexes in which the 8-$BzTT^-$ ligand is bonded to the metal by the N7. Nevertheless, a similar wrong conclusion was previously drawn for complex **2**, later corrected by the crystal structure evidence, which unequivocally showed that 8-MTT^- was S-coordinated. The similarity of reactants and reaction conditions in the formation of **2** and **3**, differing only for the sulfur substituent (Me and Bz), supports the hypothesis that also in complex **3** the thiopurine coordination occurs through the S atom.

To obtain the mixed-phosphines analogues we repeated the above described reactions of 8-TTH_2, 8-MTTH, and 8-BzTTH using the mixed phosphines precursor [RuClCp(PTA)(PPh_3)]. Complexes [RuCp(8-TTH)(PPh_3)(PTA)] (**7**), [RuCp(8-MTT)(PPh_3)(PTA)] (**8**), and [RuCp(8-BzTT)(PPh_3)(PTA)] (**9**) were obtained from each reaction as single products in good yields (Scheme 3).

The IR spectra of the complexes are in agreement with the proposed structures, the IR spectrum of **7** being the only one in which a ν(NH) absorption was observed at 3250 cm^{-1}. Additionally, the ^{1}H NMR spectrum for **7** in $CDCl_3$ showed a singlet at 9.91 ppm which can only be assigned to the N7−H proton of 8-TTH^-, suggesting that the coordination site is the deprotonated S atom.[23b] The ^{1}H NMR spectra of **8** and **9** are similar to those observed for the analogues **2** and **3**, supporting similar structures. The $^{13}C\{^1H\}$ NMR spectra of **7**, **8**, and **9** are similar to those of **1**, **2**, and **3**, respectively. The $^{31}P\{^1H\}$ NMR spectra of **7**, **8**, and **9** show two doublets due to coordinated PTA (−34.89 for complex **7**, −38.53 for **8** and −37.57 for complex **9**) and PPh_3 (51.44 ppm, 48.94 ppm and 48.80 ppm for **7**, **8**, and **9**) coupled each other with $^2J_{PP}$ = 40.52 Hz in complex **7**, $^2J_{PP}$ = 38.42 Hz in complex **8**, and $^2J_{PP}$ = 37.71 Hz in complex **9**. The data for the starting complex [RuClCp(PTA)(PPh_3)] are similar

Chart 3

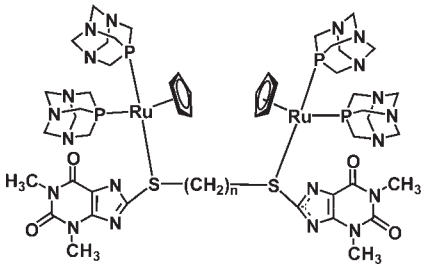

n = 1, (**4**)

n = 2, (**5**)

n = 3, (**6**)

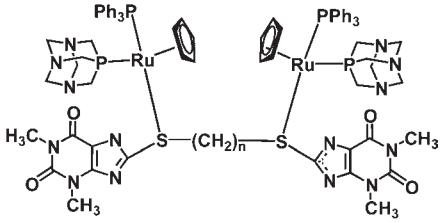

n = 1, (**10**)

n = 2, (**11**)

n = 3, (**12**)

[−34.96 and 48.16 ppm ($^2J_{PP}$ = 34.7 Hz)] showing that the phosphorus environment is not much affected by the nature of the anionic ligand. The proposed structure for **7**, **8**, and **9** is similar to that found for complex **2** where the thiopurinic anionic ligand is S-coordinated to the metal, which completes its coordination sphere binding to a η^5-Cp, one PTA, and one PPh_3 (Scheme 3).

The obtained mononuclear products **1**− **3** and **7**−**9** are air stable for months in the solid state, while solutions in water (complexes **1**−**3**) or $CDCl_3$ (complexes **7**−**9**) are stable for more than 2 days.

Binuclear Complexes Containing Bis-Thiopurines: Synthesis of 4, 5, 6 and 10, 11, 12. The reactions of $MBTTH_2$, $EBTTH_2$, and $PBTTH_2$ (**d-f**, Chart 1) with 2 equiv of KOH in H_2O and 2 equiv of [RuClCp(PTA)$_2$] gave the binuclear complexes **4**, **5**, and **6**, while the same ligands with 2 equiv of KOH and 2 equiv of [RuClCp(PTA)(PPh$_3$)] in EtOH produced **10**, **11**, and **12**. (Chart 3). The obtained binuclear products are air stable in solid state for months as well as solutions of **4**− **6** in water, of **10** and **12** in $CDCl_3$ and of **11** in DMSO are air stable for more than 2 days.

For every product, the elemental analysis was in agreement with a proportion of two $\{CpRuLL'\}^+$ (L = PPh_3, PTA; L′ = PTA) units to one bis-thiopurine molecule. The $^{31}P\{^1H\}$ NMR spectra of complexes **4**, **5**, and **6** show a singlet at −22.16 ppm, −22.41 ppm, and −25.34 ppm, respectively, similar to those found for the monothiopurine Cp-PTA ruthenium complexes **1**−**3**. Complexes **10**, **11**, and **12** display two doublets reciprocally coupled due to PTA and PPh_3 bonded to the same metal nucleus [**10**: −34.96 ppm, 51.36 ppm (d, $^2J_{PP}$ = 40.58 Hz); **11**: −37.78 ppm, 50.17 ppm (d, $^2J_{PP}$ = 38.71 Hz); **12**: −38.53 ppm, 48.21 ppm (d, $^2J_{PP}$ = 38.52 Hz)]. The ^1H NMR signals of **4**, **5**, and **6**, and **10**, **11**, and **12** were assigned by the use of ^1H, ^1H-2D COSY NMR and were found to be similar to those of the corresponding mononuclear analogues **1**−**3** and **7**−**9**, plus the signals of the linking CH_2 chain of the bis-thiopurines. The $MBTTH_2$ S-CH_2-S group in **10** was found as a broad singlet at 4.62 ppm, which is in the range to that found for the complexes *cis*-[{PtCl(PPh$_3$)$_2$}$_2$(μ-MBTT-$\kappa N7,N7'$)] (5.0 ppm), *cis*-[{Pt(PTA)$_2$}$_2$(μ-Cl)(μ-MBTT-$\kappa N7,N7'$)]Cl (4.21 ppm),[18] and *trans*-[{PdCl(PPh$_3$)$_2$}$_2$(μ-MBTT-$\kappa N7,N7'$)] (4.15 ppm).[22] Nevertheless, in the ^1H NMR spectrum of **4**, it was not possible to locate the S-CH_2-S hydrogen atoms, whose signal is probably overlapped to the H_2O residue signal. Moreover, in the $^{13}C\{^1H\}$ NMR spectra of **4** and **10** the chemical shifts of S-CH_2-S and C8 signals (**4**: δ S-CH_2-S = 38.07, C8 = 153.83 ppm; **10**: δ S-CH_2-S = 33.95, C8 = 151.85 ppm) are very close to those found in *cis*-[{Pt(PTA)$_2$}$_2$(μ-Cl)(μ-MBTT-$\kappa N7,N7'$)]Cl (δ S-CH_2-S = 35.85, C8 = 150.52 ppm) and *trans*-[{PdCl(PPh$_3$)$_2$}$_2$(μ-MBTT-$\kappa N7,N7'$)] (δ S-CH_2-S = 36.90, C8 = 150.30 ppm).

The comparative analysis of the ^1H NMR spectra of the complexes **5** and **11** was very useful for the right assignment of their signals that was only possible as both complexes are soluble in DMSO-d_6. In complexes **5** and **11** the four S-$(CH_2)_2$-S protons are chemically different and arise as multiplets (**5**: 3.17, 3.39, 3.41, 3.44 ppm; **11**: 2.72, 2.95, 3.06, 3.62 ppm), while a broad singlet was observed for this group in the few known $EBTT^{2-}$ metal complexes *trans*-[{PdCl(PPh$_3$)$_2$}$_2$(μ-EBTT-$\kappa N7,N'7$)] (δ S-$(CH_2)_2$-S: 2.87 ppm)[22] and *cis*-[{Pt(PTA)$_2$}$_2$(μ-Cl)(μ-EBTT-$\kappa N7,N7'$)]Cl (δ S-$(CH_2)_2$-S: 1.92 ppm).[18] All the S-$(CH_2)_2$-S protons present an individual signal and the large range of their chemical shifts suggest that the coordination of the ligand to the metal has a large influence on this group. Therefore, it is more likely that the coordination of the $EBTT^-$ ligand occurs through the S atom, directly bonded to -CH_2-CH_2-, than through the quite distant N7. In the $^{13}C\{^1H\}$ NMR spectra of **5** and **11** the chemical shift of the S-$(CH_2)_2$-S and C8 signals (**5**: δ S-$(CH_2)_2$-S = 34.74, C8 = 151.68 ppm; **11**: δ S-$(CH_2)_2$-S = 32.38, C8 = 150.67 ppm) are similar to those of free $EBTTH_2$ (δ S-CH_2-S = 32.00, C8 = 148.10 ppm) and of the reported complexes *cis*-[{Pt(PTA)$_2$}$_2$(μ-Cl)(μ-N,N-EBTT)]Cl (δ S-$(CH_2)_2$-S = 35.85, C8 = 150.52 ppm) and *trans*-[{PdCl(PPh$_3$)$_2$}$_2$(μ-EBTT-$\kappa N7,N'7$)] (δ S-$(CH_2)_2$-S = 32.70, C8 = 150.90 ppm).

In complexes **6** and **12** the S-$(CH_2)_3$-S ^1H NMR signals arise as multiplets at distinct chemical shifts (**6**: δ -CH_2- = 1.56 ppm, δ S-CH_2- = 2.95, 4.64 ppm; **12**: δ -CH_2- = 2.20 ppm, δ S-CH_2- = 3.22, 4.48 ppm) quite different from those of the free $PBTTH_2$ (δ -CH_2- = 2.17, S-CH_2- = 3.40 ppm) and of coordinated $PBTT^{2-}$ in *cis*-[{Pt(PTA)$_2$}$_2$(μ-Cl)(μ-PBTT-$\kappa N7,N'7$)]Cl (δ -CH_2- = 2.03, S-CH_2- = 3.39 ppm)[22] and *trans*-[{PdCl(PPh$_3$)$_2$}$_2$(μ-PBTT-$\kappa N7,N'7$)] (δ -CH_2- = 2.56, S-CH_2- = 3.72 ppm).[18] This fact suggests once more that the S atom is the coordination point of the $PBTT^-$ ligand in **6** and **12**. The compounds **6** and **12** display a similar $^{13}C\{^1H\}$ NMR spectra except for the PPh_3 signals. In particular, the chemical shifts of the bridging -CH_2- and of C8 carbon atoms are similar in **6**

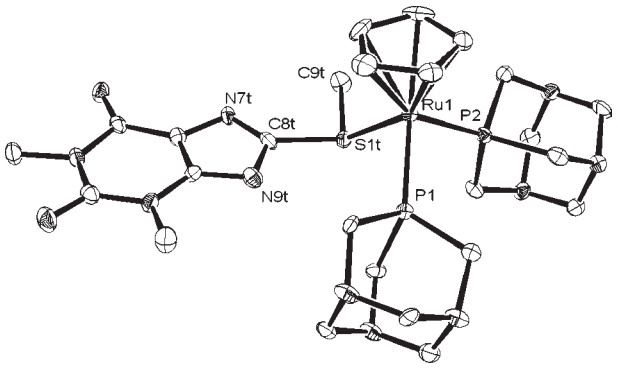

Figure 1. ORTEP view of compound **2** with atom numbering scheme showing 50% probability thermal ellipsoids. For the sake of clarity the H atoms were omitted.

(δ -CH_2-, S-CH_2-, C8 = 28.30, 45.87, 149.73 ppm) and **12** (δ -CH_2-, S-CH_2-, C8 = 30.23, 44.11, 152.06 ppm). If these values are compared with those found for free $PBTTH_2$ (δ -CH_2-, S-CH_2-, C8 = 29.20, 30.20, 148.20 ppm) and for the reported complexes *cis*-[{Pt(PTA)$_2$}$_2$(μ-Cl)(μ-PBTT-$\kappa N7,N'7$)]Cl[18] (δ -CH_2-, S-CH_2-, C8 = 32.00, 32.20, 151.86 ppm) and *trans*-[{PdCl(PPh$_3$)$_2$}$_2$(μ-PBTT-$\kappa N7, N'7$)][22] (δ -CH_2-, S-CH_2-, C8 = 28.60, 30.40, 151.00 ppm), a substantial invariance is found for δ -CH_2- and δ C8, while the S-CH_2- chemical shift found in **6** (45.87 ppm) and **12** (44.11 ppm) is about 14 ppm shifted with respect to the same signal in free $PBTTH_2$ (30.20 ppm) and in Pt/Pd-$PBTT^{2-}$ complexes (32.20 and 30.40 ppm, respectively). This remarkable difference, in our opinion, is another NMR-based evidence supporting the hypothesis of S-coordination versus N-coordination.

Because of the poor quality of the crystals resulting from many recrystallization attempts, it was not possible to obtain any X-ray structure for binuclear complexes containing bis-8-thio-theophyllines. However, the spectroscopic evidence support the structures reported in Chart 3 as the most probable for complexes **4**−**6** and **10**−**12**, where each S of the bis-8-thio-theophylline derivative is bonded to a Ru, which completes its coordination geometry with an η^5Cp and two phosphines.

Crystal Structure of [RuCp(8-MTT-κS)(PTA)$_2$]·4H$_2$O (2·4H$_2$O). Single crystals good for X-ray determination of **2** were obtained by slow evaporation from its solution in EtOH. An ORTEP[29] view is displayed in Figure 1, the crystallographic data are given in Table 1, and a list of selected bond distances and angles appears in Table 2.

The asymmetric unit contains four disordered H_2O molecule and one chiral neutral [RuCp(8-MTT-κS)-(PTA)$_2$] molecule (Figure 1). The metal is coordinated with a slightly distorted pseudo-octahedral geometry to one η^5-Cp, two PTA ligands bonded by the P atom, and one 8-MTT^- ligand through the S atom. The distortion of the coordination geometry in **2** (P1−Ru−P2 = 94.17(5)°; P1−Ru−S1t = 90.18(4)°; P2−Ru−S1t = 89.32(4)°) is shorter than that in the starting complex [RuClCp(PTA)$_2$] (P1−Ru−P2 = 96.85°; P1−Ru−Cl = 91.61(7)°; P2−Ru−Cl = 86.46(7)°).[30] The atomic radius of S and Cl are nearly similar and therefore the shorter geometrical distortion in **2** with respect to [RuClCp(PTA)$_2$] is only able to be attributed to the effect of the entire 8-MTT^- ligand as a whole.

Table 2. Selected Bond Distances (Å) and Angles (deg) for **2**

Ru1−P1	2.2665(12)
Ru1−P2	2.2722(13)
Ru1−S1t	2.3515(12)
Ru1−$Cp_{(centroid)}$	1.865(5)
S1t−C9t	1.808(5)
S1t−C8t	1.792(5)
C8t−N7t	1.308(7)
C8t−N9t	1.376(6)
P1P−C3P	1.856(10)
P1−Ru1−P2	94.17(5)
P1−Ru1−S1t	90.18(4)
P2−Ru1−S1t	89.32(4)
C8t−S1t−Ru1	113.00(17)
C9t−S1t−Ru1	109.72(18)
S1t−C8t−N7t	122.9(4)
S1t−C8t−N9t	116.8(4)

The Ru−$Cp_{centroid}$ distance is 1.865 Å that is larger than that observed in the starting complex [RuCpCl-(PTA)$_2$] (Ru−$Cp_{centroid}$ = 1.844 Å)[30] while the bond lengths between the ruthenium atom and both PTA phosphorus atoms (Ru−P1 = 2.266(1) Å; Ru−P2 = 2.272(1) Å) are different to those observed in the starting complex: respectively 2.258(3) Å and 2.247(3) Å. Surprisingly, the 8-MTT^- anion is not coordinated by the purine-N7 atom, which was the expected coordination position as observed in most of the until now known crystal structures of purine-metal complexes, but by the purine-thio-ether-S atom.[17,22,23] Although there are several examples of bonds between Ru atoms and thioether S atoms, there are only three examples of ruthenium complexes containing nitrogen-thioether ligands,[31] but none of them contains the ligand exclusively coordinated by sulfur. Additionally, there are no examples of complexes containing thioether-purines or other thioethers bearing NH groups, competing for coordination on the metal or stabilizing the S-thio-ether coordination by the formation of a chelate ring. This unexpected coordination mode could be because the S bonded compound is lower in energy than the N bonded, for steric reasons. Preliminary theoretical studies on the interaction between thio-purines and {CpRuPTA} moieties support this idea; nevertheless an extensive theoretical and experimental study is in progress, which will be presented in a future paper.

The distance Ru−S1 (2.3515(12) Å) in **2** is shorter than that found in [Ru(*N*,*N*-dps)$_2$(*N*,*S*-c)][PF_6]$_2$·C_3H_6O (Ru−S = 2.370(1) Å),[31b] its isomer [Ru(*N*,*N*-dps)$_2$(*N*,*S*-dps)](PF_6)$_2$·H_2O (Ru−S(3) = 2.424(2) Å), and [Ru(dps-N,N′)$_2$pmprs](PF_6)$_2$·C_2H_3N (Ru1−S34 = 2.3581(13) Å)[31a] (dps = di-2-pyridyl sulfide; c = 2-pyridymethyl 2-pyridyl sulfide; pmprs = 4-methylpyrimidin-2-yl 2-pyridylmethyl sulfide). Until now, the crystal structure of [Ru(8-MTT-$\kappa N7,O6$)$_2$(PPh_3)$_2$][32] is the only known ruthenium complex containing a 8-MTT^- ligand coordinated

(29) Johnson, C. K. *ORTEP II. Report ORNL-5138*; Oak Ridge National Laboratory: Oak Ridge, TN, 1976.

(30) Frost, B. J.; Mebi, C. A. *Organometallics* **2004**, *23*, 5317–5323.

(31) (a) Baradello, L.; Lo Schiavo, S.; Nicolò, F.; Lanza, S.; Alibrandi, G.; Tresoldi, G.; Nicolo, F.; Lanza, S. *Acta Crystallogr., Sect.C: Cryst. Struct. Commun.* **2005**, *C61*, m169–m172. (b) Baradello, L.; Lo Schiavo, S.; Nicolo, F.; Lanza, S.; Alibrandi, G.; Tresoldi, G. *Eur. J. Inorg. Chem.* **2004**, 3358. (c) Scopelliti, R.; Bruno, G.; Donato, C.; Tresoldi, G. *Inor. Chim. Acta* **2001**, *313*, 43–55.

(32) Mañas Carpio, S. Ph.D. Dissertation, University of Almería, Almería, Spain, 2003.

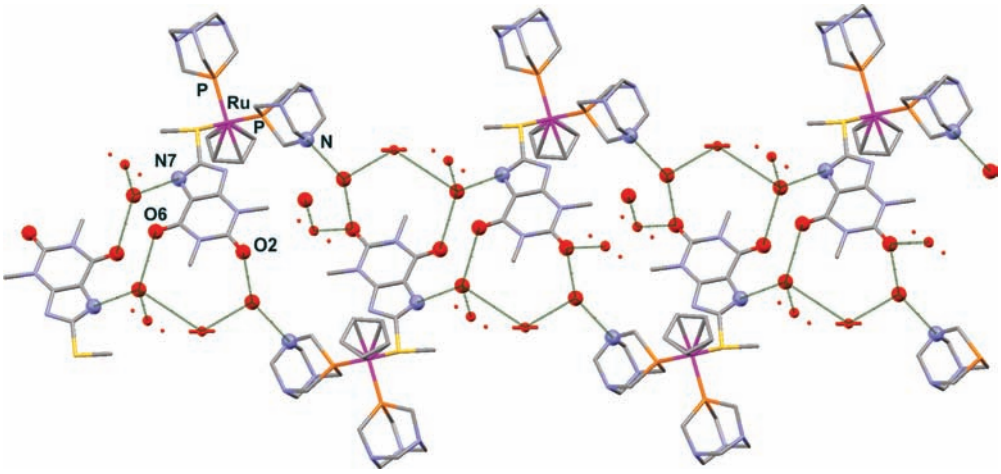

Figure 2. Hydrogen bond network produced by the interaction of the disordered H_2O molecule, the N7, O2, O6, and N1 atoms of **2**.

to a Ru atom. In this complex the ligand 8-MTT$^-$ is coordinated to the metal by O6 and the deprotonated N7 atom. The C8−S1 and S1−CH_3 distances in this complex (C8−S1 = 1.755(4) Å; S1−CH_3 = 1.770(5) Å) are significantly shorter (ΔC8−S = 0.037 Å; ΔS−CH_3 = 0.038 Å) than those for **2** (S1t−C8t = 1.792(5) Å; S1t−C9t = 1.808(5) Å). Additionally, the bond lengths between C8 and the imidazolic nitrogen atoms N7 and N9 in **2** are quite different (C8t−N7t = 1.308(7) Å; C8t−N9t = 1.376(6) Å) in comparison with the distance C8−N7 and C8−N9 in the complex [Ru(8MTT-$\kappa N7$,$O6$)$_2$-(PPh_3)$_2$] (C8−N7 = 1.338(4) Å; C8−N9 = 1.377(5) Å) and the other known MTT$^-$ metals complexes and N7 coordinate purine metal complexes.[17] The crystal structure of $MBTTH_2$ is the only one known for a free 8-thioteophilline derivative.[22] The bond C8−S and S−CH_2-distances in both sides of the molecule are the same (S1A−C8A = 1.749(2) Å; S1B−C8B = 1.748(2) Å; S1A−C10 = 1.807(2) Å; S1B−C10 = 1.816(2) Å) and quite similar to those bond lengths in **2**. Nevertheless, the C8−N7 and C8−N9 (C8A−N7A = 1.353(3) Å; C8A−N9A = 1.339(2) Å; C8B−N7B = 1.359(2) Å; C8B−N9B = 1.345(2) Å) are rather different to those found for **2**. It is important to point out that the average distance between C8−N7 and C8−N9 in **2** (1.342(7) Å) is the same than that found in $MBTTH_2$ (1.346(3) Å) but different than that for [Ru(8MTT-$\kappa N7$,$O6$)$_2$(PPh_3)$_2$] (1.357(5) Å). This fact suggests that the electrons in the skeleton of complex **2** are mainly located between the N7−C8−S−Ru atoms, with a particular high-density charge on the N7−C8 and on the S−Ru bond. Therefore the electrons coming from the deprotonation of the N7 atom are finally located on the S8 atom, which is the donor site of the ligand.

The purine is planar, the distance between the purine plane and the S, C9t, P1, and P2 being 0.243, 0.08, 0.134, and 0.160 Å, respectively. The purine and Cp are almost parallel as the angle between them is 4.14°. The MTT$^-$ disposition avoids repulsive interactions with the rest of the molecule, as the distances among the purine and the others ligands in the complex are longer than 3 Å. A 3D network through extensive hydrogen bonding involving the disordered H_2O molecule, the N7, O2, O6, and N1 atoms forms the crystal lattice structure (Figure 2).

Table 3. Estimated IC50 on *cisplatin*-Sensitive T2 Cell Line, *cisplatin*-Resistant SKOV3, and Partition Coefficient Log *P* of **1**−**3**, **7**−**8**, [RuClCp(PTA)$_2$], and [RuClCp(PPh_3)(PTA)]

complex	T2	SKOV3	Log *P*
[RuClCp(PTA)$_2$]	> 50 μM	> 50 μM	−1.85
1	> 50 μM	> 50 μM	−1.29
2	> 50 μM	> 50 μM	−1.41
3	> 50 μM	> 50 μM	−0.97
[RuClCp(PPh_3)(PTA)]	10−50 μM	> 50 μM	0.75
7	∼50 μM	> 50 μM	0.96
8	∼50 μM	> 50 μM	1.26
9	2−10 μM	> 50 μM	1.54

Cell Growth Inhibition. The mononuclear complexes **1**−**3** and **7**−**9** have been tested for cell growth inhibition activity on two human cancer cell lines: the *cis*platin-sensitive T2 (results reported in Table 3) and the *cis*platin-resistant SKOV3 (results reported in Table 3). In the tests the growth inhibition activity values of the precursors [RuClCp(PPh_3)(PTA)] and [RuClCp(PTA)$_2$] were acquired for comparison. Each complex was dissolved in DMSO and diluted in AIM-V medium to obtain the final concentrations of 50, 10, and 2 μM solutions. The chemical stability of the complexes in water/DMSO solutions was verified by $^{31}P\{^1H\}$ NMR over 2 weeks. The percentage of growth inhibition at the three doses for each complex allowed us to estimate the IC50, the concentration reducing to 50% the cell growth of both cell lines (Table 3).

Tests with the *cis*platin-sensitive cells T2 show that complexes containing one PTA and one PPh_3 (**7**−**9** and the precursor [RuClCp(PPh_3)(PTA)]) display a significantly better activity than those containing two PTA (**1**−**3**), whose activity is very low, including the precursor [RuClCp(PTA)$_2$]). This fact has been observed before with PTA-Pt complexes, and it is probably related to the difficulty for hydrophilic PTA complexes in crossing the lipophilic membranes of the cell and of the nucleus to reach their target, the nucleic acids. To give support to this hypothesis, we determined the partition coefficient Log *P* for each complex, and we found a good correlation between Log *P* and the antiproliferative activity. The data in Table 3 indicate that the highest value for Log *P* was found for complex **9**, which present also the highest cell growth inhibition activity, comparable to *cis*platin

(IC50 = 2−10 μM). The found data support the hypothesis that the liphophilic/hydrophilic balance could be a determining factor for the biological activity trend inside the group of the Ru complexes examined in this paper.

Tests with the *cis*platin-resistant SKOV3 cell line show that all the tested complexes are inactive like *cis*platin (IC50 = > 50 μM) on the Pt-resistant cell line. This observation supports the hypothesis that complex **9**, as active as *cis*platin on Pt-sensitive cells and as inactive as *cis*platin on Pt resistant cell line, is likely operating by the same mechanism as classical Pt containing drugs.

The values for dinuclear complexes **4**−**6** and **10**−**12** are not reported because preliminary tests indicated poor activity and therefore were abandoned.

Conclusion

Two groups of new organometallic Ru(II) complexes have been prepared and characterized: the first is composed by mononuclear neutral complexes where Ru is bonded to Cp, to two phosphines (two PTA or one PTA and one PPh_3), and to the deprotonated form of one of the thiopurines **a-c**, depicted in Chart 1. The second group includes binuclear complexes with a bis-thiopurine (**d-f** in Chart 1), in its dianionic form, connecting two $\{CpRu(PR_3)_2\}$ (PR_3 = PTA, PPh_3) groups. The crystal structure of complex **2** showed that the thiopurinate is S-coordinated. This is the first example of a single S-coordinate thioether-amine and S-coordinated thiopurinate, invariably found N7-coordinated even with soft metals like Pt, Pd, and Au. All the reactions producing complexes **1**−**12** occur with complete regioselectivity, and the spectroscopic data support the hypothesis that all the isolated products contain exclusively S-coordinated thiopurines.

The antiproliferative activity of the Ru complexes **1**−**12** on model tumoral cell lines (T2 and SKOV3) has been tested. It was found that complex **9** shows an activity comparable with *cis*platin on T2 and no activity on SKOV3, indicating that its antiproliferative activity is likely to be related to a *cis*platin-like mechanism. While the other complexes showed a poor bioactivity, the notable result of **9** is probably due to the most favorable hydrophilicity/lipophilicity balance, reached with its combination of ligands, associating one hydrophilic PTA with lipophilic groups like PPh_3 and the thiopurine substituent CH_2Ph.

Acknowledgment. Funding is provided by Junta de Andalucía through PAI (research teams FQM-317) and Excellence Projects FQM-03092, MCYT (Spain) by project CTQ2009-10538 and the COST Action CM0802 (WG2, WG3, WG4).

Supporting Information Available: Further details about the synthesis for compounds **1**−**12**. This material is available free of charge via the Internet at http://pubs.acs.org. Crystallographic data for the structures in this paper have been deposited with the Cambridge Crystallographic Data Centre as supplementary publications nos. CCDC 785135. Copies of the data can be obtained, free of charge on applications to CCDC, 12 Union Road, Cambridge CB2 1EZ, U.K., (fax: +44 1223 336033 or e-mail: deposit@ccdc.cam.ac.uk).

Note Added after ASAP Publication. This paper was published on the Web on January 12, 2011, with the author name Canella misspelled. The corrected version was reposted on January 31, 2011.